Surface Diffusion in C_{18}-Silica Monolithic Stationary Phase

Kanji Miyabe
Graduate School of Science and Engineering for Research, University of Toyama, 3190, Gofuku, Toyama 930-8555, Japan

Abstract

A peak parking–moment analysis method was used for the measurement of surface diffusion coefficient (D_s) in a reversed-phase liquid chromatography (RPLC) system consisting of a C_{18}-silica monolithic column and a mixture of methanol and water (70/30, v/v). The D_s values experimentally measured were analyzed by considering the correlation with corresponding values of molecular diffusivity (D_m) and the retention equilibrium constant (K_a). It seems that the correlation between D_s/D_m and K_a is represented by a single curve irrespective of the RPLC conditions of temperature and the type of sample compounds. The increase in K_a is accompanied with the decrease in D_s/D_m. Oppositely, the ratio of D_s/D_m increases and approaches around unity when K_a infinitely decreases. It seems that surface diffusion is originally similar to molecular diffusion and that it is restricted due to the sample retention. These characteristics of surface diffusion are the same between the C_{18}-silica monolithic stationary phase and the conventional C_{18}-silica gel particles. In addition, the values of K_a and D_s are also comparable between them. It is concluded that basic properties concerning the retention equilibrium and surface diffusion of the C_{18}-silica monolithic stationary phase are almost the same as those of the conventional C_{18}-silica gel particles in spite of the difference between their structural characteristics.

Introduction

It is the demand of the time to develop fast high-performance liquid chromatography (HPLC) with high efficiency. Monolithic separation media have abundantly been studied as a powerful tool for this purpose (1–8). Among the various monolithic media, a C_{18}-silica monolithic column is probably one of the most popular packing materials for reversed-phase liquid chromatography (RPLC). It is well recognized that, compared with conventional columns packed with spherical silica gel particles, silica monolithic columns have different properties of chromatography (i.e., high permeability and separation efficiency under high flow rate conditions). These advantages originate from the structural characteristics of silica monolithic media, which have a through-macropore network with high external porosity and thin threads of porous silica skeleton. These structural characteristics, respectively, contribute to the reduction of hydraulic resistance to the mobile phase flow and the enhancement of mass transfer of sample molecules in the stationary phase. The advantageous separation efficiency of the silica monolithic media is essentially correlated with mass transfer kinetics in the stationary phase. However, there are not so many fundamental studies on the intrinsic characteristics of monolithic separation media from kinetic points of view. Although there have been a great number of publications, most of them are relating to chromatographic separations with monolithic columns for various applications.

Glossary

d_p	particle diameter, μm
D	diffusivity, $cm^2\ s^{-1}$
$D_{ax,m}$	axial dispersion coefficient of sample molecules in the mobile phase, $cm^2\ s^{-1}$
$D_{ax,s}$	axial dispersion coefficient of sample molecules in the stationary phase, $cm^2\ s^{-1}$
$D_{ax,t}$	total axial dispersion coefficient of sample molecules, $cm^2\ s^{-1}$
D_{Ls}	diffusion coefficient defined in Equation 6, $cm^2\ s^{-1}$
D_m	molecular diffusivity, $cm^2\ s^{-1}$
D_s	surface diffusion coefficient, $cm^2\ s^{-1}$
$J_{ax,s}$	flux of sample molecules due to axial molecular diffusion in the stationary phase, $g\ cm^{-2}\ s^{-1}$
J_s	flux of sample molecules due to surface diffusion in the stationary phase, $g\ cm^{-2}\ s^{-1}$
k	retention factor
K_a	retention equilibrium constant
M_w	molecular weight
N_c	number of carbon atom in the side chain of sample molecule
q	amount of sample molecules adsorbed, $g\ cm^{-3}$
r	radial distance from particle center, cm
t_p	peak parking time, s
T	absolute temperature, K
V_e	elution volume, cm^3
z	longitudinal distance from inlet of column, cm

Greek letters

γ_m	obstructive factor
ε_e	external porosity
ε_i	internal porosity
ε_t	total porosity
η	viscosity, Pa s
μ_1	first absolute moment, s
μ_2'	second central moment, s^2
$\sigma_{ax,mol}^2$	total variance due to axial molecular dispersion in both the mobile and stationary phases, cm^2

Peak spreading in columns has frequently been studied by using ordinary rate equations because it is an important subject in chromatography (9–13). The moment analysis (MA) theory based on the general rate model of chromatography has also been applied to the kinetic subject (10,14,15). It is usually assumed that the band broadening is attributed to the contributions of several mass transfer processes in the column (i.e., axial dispersion, external mass transfer, intra-stationary phase diffusion, and real adsorption/desorption kinetics). Among them, the mass transfer phenomena in the stationary phase must be studied in detail because it has a significant influence on the column efficiency under high flow-rate conditions. In addition, it has been reported that surface diffusion plays a quite important role for the mass transfer in the stationary phase (16–18). This means that fundamentals of surface diffusion should be studied in detail for well understanding some intrinsic characteristics of chromatographic behavior of monolithic separation media.

In 1964, Knox and McLaren (19) introduced a new method for determining diffusion coefficient and obstructive factor in gas chromatography (GC). It is called "stopped flow method", "arrested flow method", and "peak parking method" (PP). They injected ethylene as an unretained tracer into a column and continued the GC procedure until it reaches around the middle part of the column. Then, the band elution was stopped for a while to allow the sample band to spread by diffusion in the axial direction of the column. After the interruption, the carrier gas (nitrogen) flow was resumed to elute the sample band from the column, of which the width was measured. They determined the diffusion coefficient of ethylene in nitrogen as 1.65×10^{-1} cm^2 s^{-1} at 291 K and 100 kP$_a$ and the obstruction factor between 0.46 and 0.74 for different GC packing materials from the systematic measurements of the peak width as a function of the interruption period.

The arrested flow or stopped flow method has been used for some kinetic properties in various GC and LC systems (20–25). Recently, the PP–MA method has also been applied to the kinetic study on the mass transfer in RPLC systems using C_{18}-silica monolithic columns and conventional columns packed with full-porous C_{18}-silica spherical particles (26–29). The information about intraparticulate mass transfer kinetics can be derived from the band broadening due to axial diffusion during the interruption period. It is demonstrated on the basis of experimental data that the same values of D_s can be obtained by the PP–MA method and the pulse response (PR)–MA method, which is an effective strategy for the kinetic study on the mass transfer, including surface diffusion in chromatography (16–18). The D_s values also exhibit the same dependence on the retention strength (27,28). In the PP experiment, the band broadening takes place under equilibrium conditions of the sample distribution between the mobile and stationary phases because there is no convective flow during the interruption. The experimental conditions are oppositely different from those of the PR method, in which measurements of elution peaks are intentionally carried out under non-equilibrium conditions due to high flow velocities of the mobile phase.

It is the goal of this study to experimentally measure D_s values in C_{18}-silica monolithic stationary phase by using the PP–MA method and to compare the values of D_s with those measured for C_{18}-silica spherical particles. There have been semantic discussions about the retention mechanism in RPLC (i.e., "partition" or "adsorption"). However, it is not intended in this paper to discuss the retention mechanism. It is regarded as adsorption phenomena in a wide sense that sample molecules migrate between the bulk mobile phase and the stationary phase surface and that the sample molecules are concentrated on the surface.

Experimental

Column and reagents

A C_{18}-silica monolithic column (50 × 4.6 mm) (Merck, Darmstadt, Germany) was used for the PP experiments. Table I lists some physico-chemical properties of the monolithic column. A mixture of methanol (HPLC-grade) and water (70/30, v/v) was used as the mobile phase solvent. Alkylbenzene homologous series (benzene–butylbenzene) were used as the sample compounds. Sample solution was prepared by dissolving the sample compound into the mobile phase solvent at the concentration of 1 mg/mL in most cases. All the sample compounds of reagent grade were used without further purification. The values of total porosity (ε_t) and external porosity (ε_e) of the column were measured by means of the inverse size exclusion chromatography (ISEC) using benzene and polystyrene standards as the probe compounds and tetrahydrofuran as the mobile phase (30). The value of the internal porosity (ε_i) of the silica skeleton was calculated from ε_t and ε_e.

Apparatus

The PP experiments were carried out by using an HPLC system (JASCO, Tokyo, Japan) consisting of a high-pressure pump (PU-2080) and a UV–vis spectrophotometric detector (UV-2085). A 7725 valve injector (Rheodyne, Cotati, CA) was

Table I. Physico-Chemical Properties of the Stationary Phases and Columns

Stationary phase	Monolith	Particle	Particle
Average particle diameter (μm)*	–	4.5	50.6
Average mesopore diameter (nm)*	13	12.8	13.3
Mesopore volume (cm^3 g^{-1})*	1	1.06	1.20
Specific surface area (m^2 g^{-1})*	300	330	361
Carbon content [% (w/v)]*	18	16.9	16.9
Total porosity, ε_t†	0.84	0.64	0.65
External porosity, ε_e†	0.68	0.38	0.35
Internal porosity, ε_i†	0.50	0.42	0.47

* Information provided by the manufacturer.
† Information experimentally measured by the ISEC method.

used for injecting the sample solution into the column. A thermostated water bath was used for keeping the column temperature at intended levels (i.e., 288, 298, and 308 K). The BOWIN software (JASCO) was used for acquiring chromatographic data.

Procedure

The PP experiments were carried out as follows. After the RPLC system was stabilized at a constant flow velocity of the mobile phase (0.5 mL/min) and at a constant temperature, a small perturbation pulse of the sample solution (10 µL) was injected into the C_{18}-silica monolithic column. Isocratic chromatography at the constant velocity was conventionally continued until the sample band reaches an approximately longitudinally middle position of the column. Then, the band elution was interrupted for a peak parking period (t_p), during which the sample band diffuses in the axial direction of the column. After t_p, the band elution was resumed under the same isocratic conditions until the elution peak profile is completely recorded. The experimental measurements of the elution peak profiles were conducted at least in duplicate or triplicate while changing the t_p value between 0–2 h.

Data analysis

The information about the retention equilibrium [i.e., the retention equilibrium constant (K_a) and the retention factor (k)] was derived from the first absolute moment (μ_1) of the elution peaks. On the other hand, the value of D_s was derived from the second central moment (μ_2') of the peaks. A brief explanation about the kinetic data analysis procedure of the PP–MA method is provided in the following. More detailed information can be found in other literature (27–29).

The sample band broadening during t_p is represented by the variance ($\sigma_{ax,mol}^2$), which originates from the axial diffusive migration of the sample molecules.

$$\sigma_{ax,mol}^2 = 2D_{ax,t}t_p \qquad \text{Eq. 1}$$

Where $D_{ax,t}$ is the total axial dispersion coefficient, which represents the sum of the contributions of molecular diffusion in the mobile and in the stationary phases. Equation 1 indicates that $\sigma_{ax,mol}^2$ is proportional to t_p. The value of $D_{ax,t}$ is calculated from the slope of the linear correlation between $\sigma_{ax,mol}^2$ and t_p. It is also represented as follows because the sample molecules axially migrate through both the mobile and stationary phases.

$$D_{ax,t} = \frac{D_{ax,m}}{1+k} + \frac{kD_{ax,s}}{1+k} \qquad \text{Eq. 2}$$

Where k is the retention factor, which represents the distribution ratio of the sample molecules between the stationary and mobile phases in equilibrium. It is reasonable to assume that the band broadening proceeds under the retention equilibrium conditions during t_p because there is no convention flow of the mobile phase in the column. On the other hand, $D_{ax,m}$ and $D_{ax,s}$ are the axial dispersion coefficients of the sample molecules in the mobile and stationary phases, respectively.

Equation 2 is rearranged as follows when $D_{ax,m}$ is assumed to be represented as the product, $\gamma_m D_m$ (9).

$$\frac{(1+k)D_{ax,t}}{D_m} = \gamma_m + \frac{kD_{ax,s}}{D_m} \qquad \text{Eq. 3}$$

Where D_m and γ_m are, respectively, the molecular diffusivity and the obstructive factor for axial molecular diffusion in the mobile phase. The value of $D_{ax,s}$ is derived from the correlation of the left-hand side of Equation 3 against k.

The contribution of axial molecular diffusion in the stationary phase ($J_{ax,s}$) to the total mass flux in the longitudinal direction of the column is represented as follows.

$$J_{ax,s} = -(1-\varepsilon_t)D_{ax,s}\left(\frac{\partial q}{\partial z}\right) \qquad \text{Eq. 4}$$

Where ε_t is the total porosity of the column, q the amount of the sample compound adsorbed, and z the longitudinal distance along the column. On the other hand, the contribution of surface diffusion (J_s) to the intraparticle mass flux is represented as follows.

$$J_s = -(1-\varepsilon_i)D_s\left(\frac{\partial q}{\partial r}\right) \qquad \text{Eq. 5}$$

Where r and ε_i are the radial distance from the center of the stationary phase particle and its porosity, respectively. The value of D_{Ls} is calculated from $D_{ax,s}$.

$$D_{Ls} = \frac{1-\varepsilon_t}{1-\varepsilon_i} D_{ax,s} \qquad \text{Eq. 6}$$

The value of D_{Ls} should be equal to that of D_s at $J_{ax,s} = J_s$. It seems that both of them represent the same flux of sample

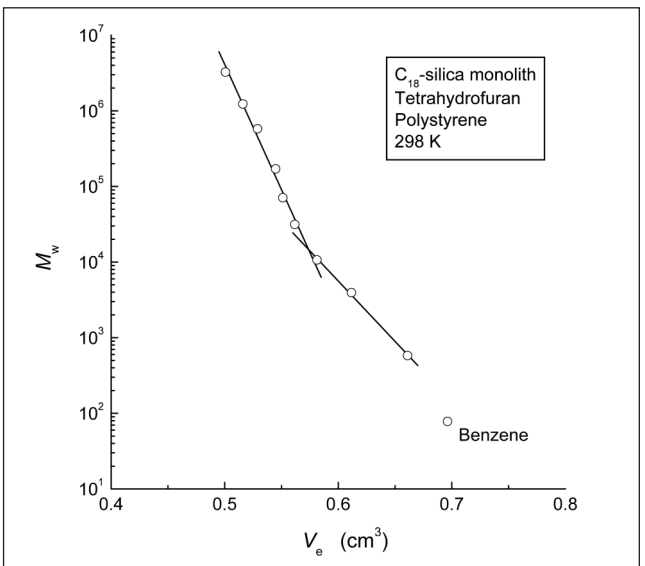

Figure 1. Correlation between M_w and V_e of polystyrene standards in SEC mode.

molecules in the stationary phase although they respectively correspond to axial dispersion and intraparticle surface diffusion. In previous papers (27–29), it has been experimentally demonstrated that D_{Ls} is equal to D_s.

Results and Discussion

Information about porosities in the column

Figure 1 illustrates the results of the ISEC experiments (30). There are two different linear correlations between the logarithmic value of molecular weight (M_w) of the probe compounds (polystyrene standards) and their elution volume (V_e). The value of ε_e was calculated as 0.68 from the intersection of the two straight lines. On the other hand, ε_t was obtained as 0.84 from the elution volume of benzene, which can penetrate all pore space in the column. Then, ε_i was calculated as 0.50 from ε_e and ε_t.

Calculation of D_s from results of the PP experiments

Figure 2 illustrates the linear correlations of the sample compounds between $\sigma_{ax,mol}^2$ and t_p at 298 K. An increase in the number of methylene unit in the side chain of the sample molecules is accompanied with the decrease in the slope of the linear lines. It is reasonably indicated that the diffusivity of large sample molecules in the longitudinal direction of the column is less than that of small molecules. According to Equation 1, the values of $D_{ax,t}$ are calculated from the slope of the straight lines. Similar PP experiments were also carried out

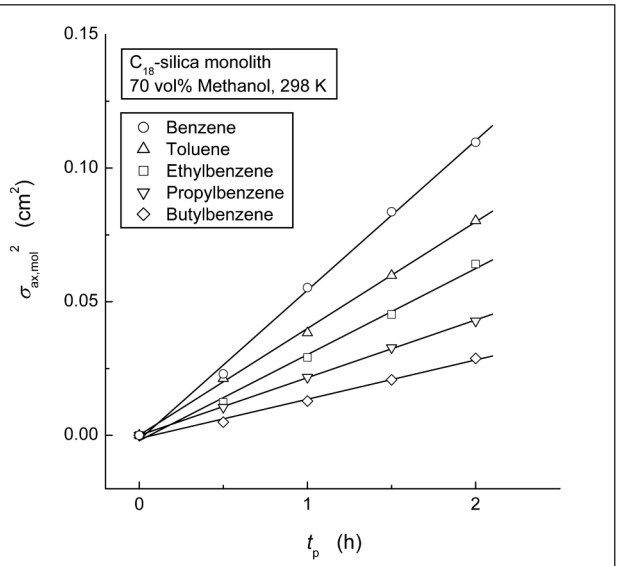

Figure 2. Correlation between $\sigma_{ax,mol}^2$ of alkylbenzene homologous compounds and t_p.

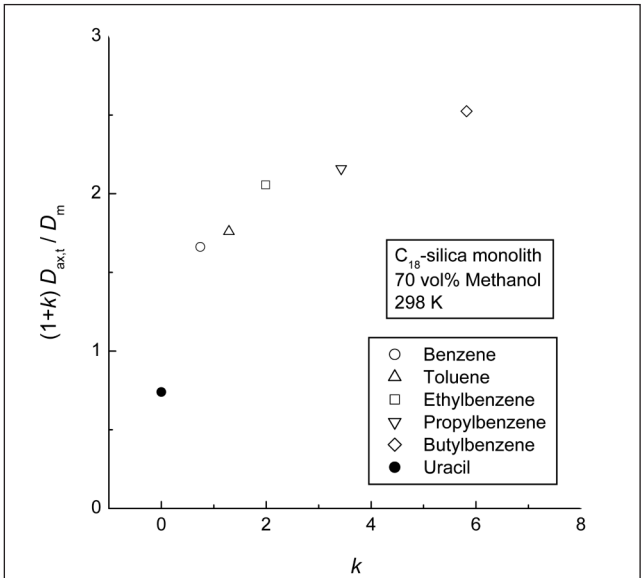

Figure 4. Correlation between $(1 + k)D_{ax,t}/D_m$ and k.

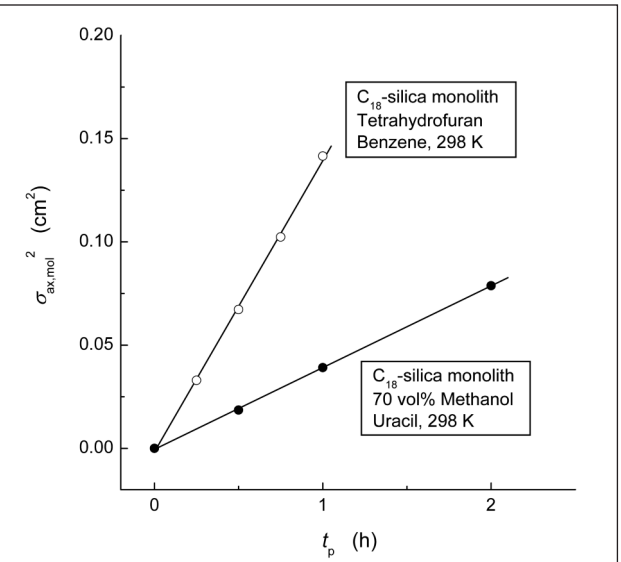

Figure 3. Correlation between $\sigma_{ax,mol}^2$ of non-retained compounds and t_p.

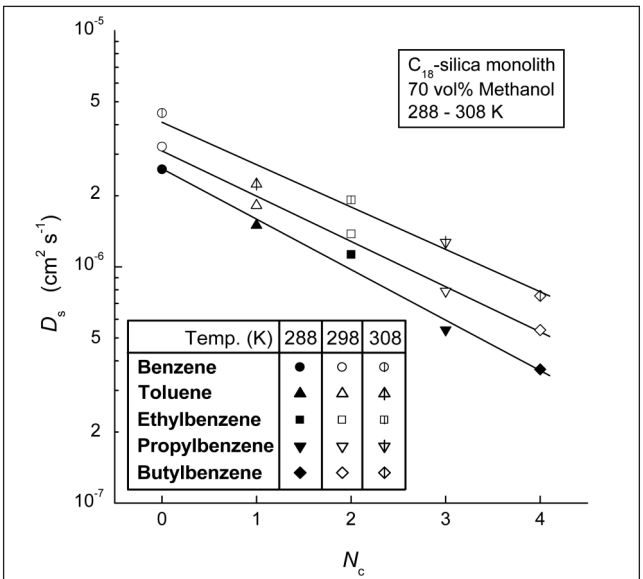

Figure 5. Correlation between D_s and N_c.

in two different systems of RPLC and SEC using uracil and benzene, respectively. They are not retained under the RPLC and SEC conditions. Again, Figure 3 illustrates the linear correlations between $\sigma_{ax,mol}^2$ and t_p at 298 K.

Figure 4 illustrates the value of the left-hand side of Equation 3 as a function of k. The solid plot at $k = 0$ indicates the value of γ_m, which was calculated as 0.74 from the slope of the linear line for uracil in Figure 3. The same value of γ_m was obtained from the linear correlation for benzene under the SEC conditions in Figure 3. Similar values have been reported for γ_m (9,19,26-29,31). Equation 3 indicates that the value of $D_{ax,s}$ is calculated from the slope of the linear line between the solid plot at $k = 0$ and each datum point. Figure 4 indicates that the value of $D_{ax,s}$ decreases with increasing k because the curved profile of the plots in Figure 4 is convex upward. The contributions of the first and second terms in the right hand side of equation 3 are compared with each other. Their contributions were calculated as 26–48% and 52–74%, respectively. The latter is 1.1 to 2.8 times larger than the former. Although the values of D_m were estimated by using the Wilke-Chang equation (32–34) in this study, the results suggest that the estimation error of D_m does not have a significant influence on the values of $D_{ax,s}$ and that accurate values of $D_{ax,s}$ are derived. Finally, Equation 6 is used for calculating D_s from $D_{ax,s}$.

Analysis of D_s values

Figure 5 illustrates the plot of D_s against the carbon number (N_c) in the side chain of the sample molecules. Although there is some scatter, the D_s value decreases with increasing N_c at each temperature. The results in Figure 5 also indicate the positive temperature dependence of D_s. This seems to be reasonable because surface diffusion is an activated process (35). Additionally, it is empirically confirmed that the ratio $D\eta/T$ is almost constant (D: diffusivity, η: viscosity, and T: temperature) (33). The empirical rule also supports the positive temperature dependence of D_s in Figure 5 because η of the mobile phase solvent decreases with increasing temperature. It is indicated in Figure 5 that the D_s value of large sample molecule is less than that of small one. This is reasonable because the diffusivity of molecules decreases with an increase in their molecular weight. On the other hand, it seems to be general in RPLC that the retention strength is oppositely enhanced with increasing sample size. The results in Figure 5 imply the dependence of surface diffusion on the retention strength. It is predicted that the retention behavior of sample molecules always affects the manner of surface diffusion because surface diffusion is molecular migration in the vicinity of the stationary phase surface under adsorbed state (14–16,35).

The value of D_s is plotted in Figure 6 as a function of the retention equilibrium constant (K_a). As predicted previously, D_s decreases with an increase in K_a. Although three different curved profiles are observed at each temperature, it can be concluded at least from the results in Figure 6 that the molecular migration by surface diffusion on the stationary phase surface is restricted by the retention of the sample molecules. However, it is hard to comprehensively analyze the results in Figure 6 because plural experimental parameters (i.e., sample compounds and temperature conditions) are simultaneously changed. In order to cancel the influence of these factors on the value of D_s, it was normalized by the corresponding value of D_m. However, roughly speaking, the value of D_s would be of the order of 1×10^{-5} cm^2 s^{-1} under weakly retained conditions in spite of the uncertainty of extrapolation. It is well recognized that the D_m values in liquid phase systems are of the order of 1×10^{-5} cm^2 s^{-1} (33).

Figure 7 illustrates the correlation of the ratio D_s/D_m with K_a. Figure 7 indicates three important characteristics of surface diffusion. At first, the ratio D_s/D_m fluctuates around a single curved line regardless of the simultaneous change in the two conditions of RPLC (i.e., temperature and the type of sample compounds). Second, D_s decreases with increasing K_a, again indicating that surface diffusion is restricted by the retention strength of the sample molecules. Finally, the ratio D_s/D_m increases and probably approaches approximate unity as K_a

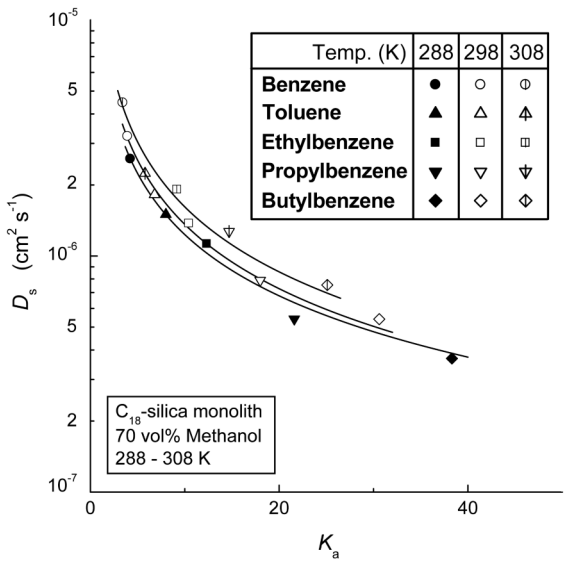

Figure 6. Correlation between D_s and K_a.

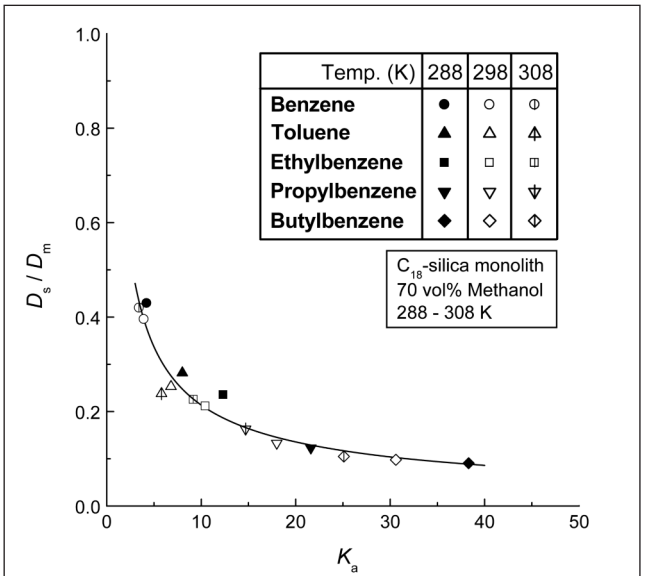

Figure 7. Correlation between D_s/D_m and K_a.

infinitely decreases, although it cannot be definitively concluded that D_s is completely equal to D_m at $K_a = 0$. This means that D_s of a weakly retained compound would be almost equal to the corresponding value of D_m. There would be an intimate correlation between surface diffusion and molecular diffusion.

The results in Figure 7 are consistent with a number of experimental observations in liquid/solid and gas/solid adsorption systems concerning the dependence of adsorption equilibrium and surface diffusion on both temperature conditions and the amount of sample compound adsorbed (14,15,35). At first, an increase in temperature is accompanied with a decrease in K_a and an increase in D_s. Second, the value of K_a decreases with an increase in the amount of the sample compound adsorbed. Oppositely, the value of D_s shows positive concentration dependence. Consequently, D_s decreases with an increase in K_a in both cases. The negative dependence of D_s on K_a seems to be a general rule.

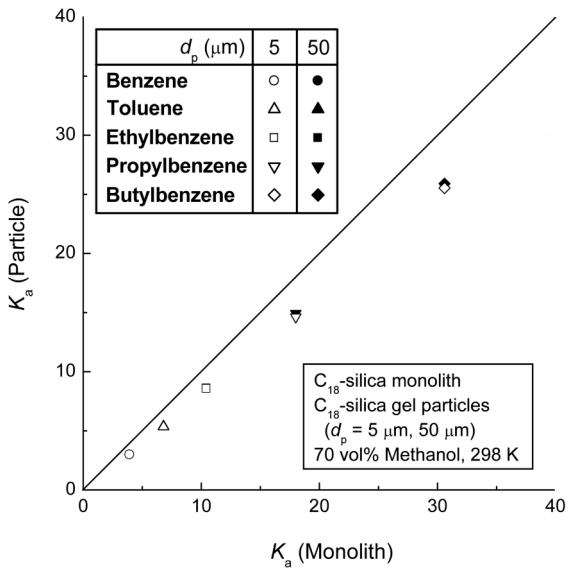

Figure 8. Comparison of K_a between C_{18}-silica monolith and C_{18}-silica gel particles.

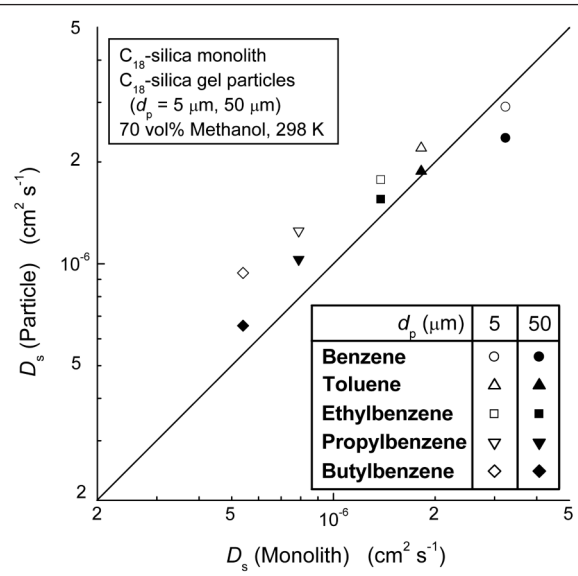

Figure 9. Comparison of D_s between C_{18}-silica monolith and C_{18}-silica gel particles.

Comparison of chromatographic behavior between monolith and particles

Figure 8 illustrates the comparison of the K_a values measured for the C_{18}-silica monolithic stationary phase and C_{18}-silica gel particles. The values of K_a are comparable with each other, suggesting that the ratio of sample concentration in the stationary phase to that in the mobile one is almost the same between the two columns. More strictly, the K_a values are 1.2–1.3 times larger for the C_{18}-silica monolithic stationary phase than for the C_{18}-silica gel particles. The slight difference between the K_a values seems to partially originate from the difference in the carbon content of the stationary phases. It is well known that the sample retention of monolithic columns is smaller than that of conventional columns packed with porous particles because of the large total porosity of monolithic stationary phases. However, Figure 8 shows that the values of K_a are comparable for the monolithic and particulate stationary phases.

On the other hand, Figure 9 illustrates the comparison of the D_s values. The plots fluctuate around the diagonal line, suggesting that the value of D_s is also comparable among the stationary phases. However, the plots do not align in parallel with the diagonal line. This means that the C_{18}-silica monolithic stationary phase is more suitable for relatively large sample compounds than for small ones. However, it is required to acquire more experimental data in order to derive a definitive conclusion.

Conclusion

The PP–MA method was applied to the kinetic study on surface diffusion in the C_{18}-silica monolithic stationary phase. The ratio D_s/D_m seems to be around unity when K_a is infinitely small, suggesting that the value of D_s of a weakly retained compound is of the same order of magnitude with D_m. This means that surface diffusion is originally similar to molecular diffusion and is restricted due to the sample retention. This conclusion for the C_{18}-silica monolithic stationary phase is the same as that for conventional C_{18}-silica particles. Silica monolithic stationary phases have some advantageous properties for fast chromatography with high efficiency in comparison with conventional particulate packing materials. However, they are attributed to its characteristic structure. There is no significant difference in the retention equilibrium and surface diffusion between the silica monolithic and particulate stationary phases.

Acknowledgments

The author is grateful to Nobuho Ando and Takuya Nakamura at the University of Toyama for their assistance to the experimental works in this study.

References

1. N. Tanaka, H. Kobayashi, K. Nakanishi, H. Minakuchi, and N. Ishizuka. Monolithic LC columns. *Anal. Chem.* **73:** 420A–429A (2001).
2. N. Tanaka, H. Kobayashi, N. Ishizuka, H. Minakuchi, K. Nakanishi, K. Hosoya, and T. Ikegami. Monolithic silica columns for high-efficiency chromatographic separations. *J. Chromatogr. A* **965:** 35–49 (2002).
3. M. Kele and G. Guiochon. Repeatability and reproducibility of retention data and band profiles on six batches of monolithic columns. *J. Chromatogr. A* **960:** 19–49 (2002).
4. A.-M. Siouffi. Silica gel-based monoliths prepared by the sol–gel method: facts and figures. *J. Chromatogr. A* **1000:** 801–18 (2003).
5. E.F. Hilder, F. Svec, and J.M.J. Fréchet. Development and application of polymeric monolithic stationary phases for capillary electrochromatography. *J. Chromatogr. A* **1044:** 3–22 (2004).
6. F. Svec. Preparation and HPLC applications of rigid macroporous organic polymer monoliths. *J. Sep. Sci.* **27:** 747–66 (2004).
7. A. Jungbauer and R. Hahn. Monoliths for fast bioseparation and bioconversion and their applications in biotechnology. *J. Sep. Sci.* **27:** 767–78 (2004).
8. G. Guiochon. Monolithic columns in high-performance liquid chromatography. *J. Chromatogr. A* **1168:** 101–68 (2007).
9. J.C. Giddings. *Dynamics of Chromatography, Part I, Principles and Theory*. Marcel Dekker, New York, NY, 1965.
10. G. Guiochon, S. Golshan-Shirazi, and A.M. Katti. *Fundamentals of Preparative and Nonlinear Chromatography*. Academic Press, Boston, MA, 1994.
11. E. Grushka, L.R. Snyder, and J.H. Knox. Advances in band spreading theories. *J. Chromatogr. Sci.* **13:** 25–37 (1975).
12. J.H. Knox. Band spreading in chromatography: a personal view. *Adv. Chromatogr.* **38:** 1–49 (1998).
13. K.H. Hamaker and M.R. Ladisch. Intraparticle flow and plate height effects in liquid chromatography stationary phases. *Separation and Purification Methods* **25:** 47–83 (1996).
14. D.M. Ruthven. *Principles of Adsorption & Adsorption Processes*. John Wiley and Sons, New York, NY, 1984.
15. M. Suzuki. *Adsorption Engineering*. Kodansha/Elsevier, Tokyo/Amsterdam, Japan/Netherlands, 1990.
16. K. Miyabe and G. Guiochon. Fundamental interpretation of the peak profiles in linear reversed-phase liquid chromatography. *Adv. Chromatogr.* **40:** 1–113 (2000).
17. K. Miyabe and G. Guiochon. Measurement of the parameters of the mass transfer kinetics in high performance liquid chromatography. *J. Sep. Sci.* **26:** 155–73 (2003).
18. K. Miyabe and G. Guiochon. Characterization of monolithic columns for HPLC. *J. Sep. Sci.* **27:** 853–873 (2004).
19. J.H. Knox and L. McLaren. A new gas chromatographic method for measuring gaseous diffusion coefficients and obstructive factors. *Anal. Chem.* **36:** 1477–82 (1964).
20. I.S. Park, J.M. Smith, and B.J. McCoy. Intraparticle diffusion coefficients in packed columns: measurement by arrested-flow gas chromatography. *AIChE J.* **33:** 1102–1109 (1987).
21. N.A. Katsanos, G. Karaiskakis, D. Vattis, and A. Lycourghiotis. Diffusion coefficients from stopped-flow gas chromatography. *Chromatographia* **14:** 695–98 (1981).
22. B.J. McCoy and A.J. Moffat. Arrested-flow chromatographic measurement of gaseous diffusion coefficients. *Chem. Eng. Commun.* **47:** 219–24 (1986).
23. M. Oh, J.M. Smith, and B.J. McCoy. Diffusion and adsorption in arrested-flow chromatography. *AIChE J.* **35:** 1224–26 (1989).
24. A.M. Striegel. Longitudinal diffusion in size-exclusion chromatography: a stop-flow size-exclusion chromatography study. *J. Chromatogr. A* **932:** 21–31 (2001).
25. B.Q. Tran, E. Lundanes, and T. Greibokk. The influence of stop-flow on band broadening of peptides in micro-liquid chromatography. *Chromatographia* **64:** 1–5 (2006).
26. H. Kobayashi, D. Tokuda, J. Ichimaru, T. Ikegami, K. Miyabe, and N. Tanaka. Faster axial band dispersion in a monolithic silica column than in a particle-packed column. *J. Chromatogr. A* **1109:** 2–9 (2006).
27. K. Miyabe, H. Kobayashi, D. Tokuda, and N. Tanaka. A kinetic parameter concerning mass transfer in silica monolithic and particulate stationary phases measured by the peak-parking and slow-elution methods. *J. Sep. Sci.* **29:** 2452–62 (2006).
28. K. Miyabe, Y. Matsumoto, and G. Guiochon. Peak parking-moment analysis. A strategy for the study of the mass-transfer kinetics in the stationary phase. *Anal. Chem.* **79:** 1970–82 (2007).
29. K. Miyabe, Y. Matsumoto, and N. Ando. Peak parking—moment analysis method for the measurement of surface diffusion coefficient. *Anal. Sci.* **25:** 211–218 (2009).
30. M. Al-Bokari, D. Cherrak, and G. Guiochon. Determination of the porosities of monolithic columns by inverse size-exclusion chromatography. *J. Chromatogr. A* **975:** 275–84 (2002).
31. E.R. Bennett and W.E. Bolch. Radioactive tracer technique for molecular diffusion coefficients in granular media. *Anal. Chem.* **43:** 55–59 (1971).
32. E.J. Wilson and C.J. Geankoplis. Liquid mass transfer at very low Reynolds numbers in packed beds. *Ind. Eng. Chem. Fundam.* **5:** 9–14 (1966).
33. R.C. Reid, J.M. Prausnitz, and B.E. Poling. *The Properties of Gases and Liquids*. McGraw-Hill, New York, NY, 1987.
34. R.B. Bird, W.E. Stewart, and E.N. Lightfoot. *Transport Phenomena*. John Wiley & Sons, New York, NY, 2002.
35. K. Kapoor, R.T. Yang, and C. Wong. Surface diffusion. *Catal. Rev. Sci. Eng.* **31:** 129–14 (1989).

Manuscript received September 15, 2008;
Revision received October 27, 2008.